Case #1

Presenter: Joy Hoang, MD

Attending: Taylor Zak, MD PhD

Clinical History:

A 78-year-old male with a history of T2DM and HTN presented to the ED due to worsening of rash and bruising of the scalp, face, upper chest, and back. The rash has been present for the past three weeks but has acutely worsened within the past few days. He reports it is itchy and painful. CT scan showed diffuse lymphadenopathy involving the axillary, mediastinal, and inguinal regions, as well as splenomegaly of up to 17 cm. Additionally, CBC shows anemia, thrombocytopenia, neutropenia, and an absolute lymphocytosis of 7.3 k/mm3. Peripheral blood smear was flagged for path review due to the presence of atypical lymphocytes. Skin biopsy of the rash, peripheral smear, and lymph node biopsy are provided for review.

Final Diagnosis: Blastic Plasmacytoid Dendritic Cell Neoplasm

Differential Diagnoses:

- Hematopoietic Neoplasms
    - Acute Myeloid Leukemia / Myeloid Sarcoma
    - Acute Undifferentiated Leukemia
    - Acute Lymphoblastic Leukemia / Lymphoma
    - Blastic Plasmacytoid Dendritic Cell Neoplasm
    - Blastoid Variant of Mantle Cell Lymphoma
- Melanoma
- Poorly differentiated carcinoma
- Merkel Cell Carcinoma
- Tumid Lupus

Histopathology:

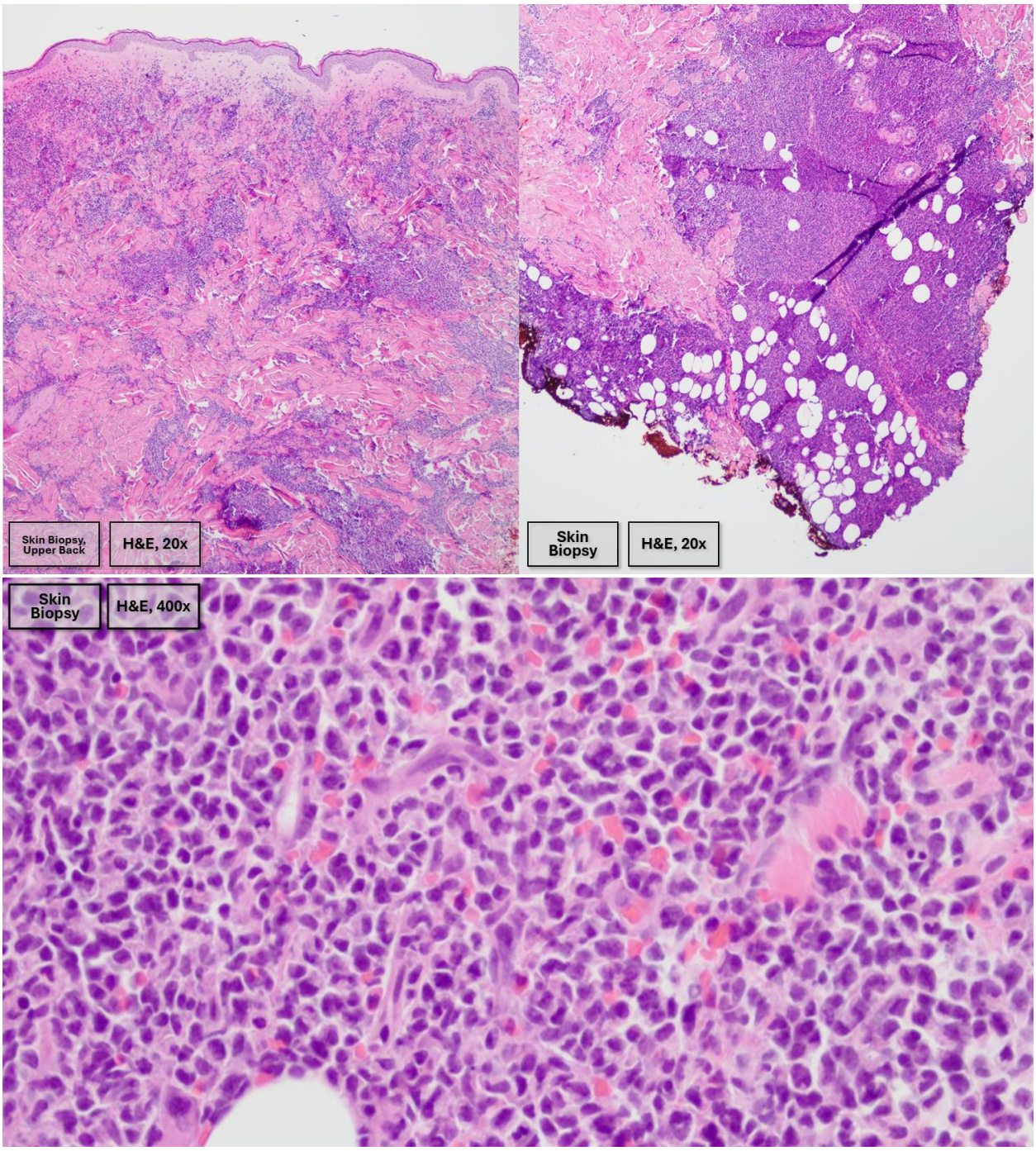

- **Skin Biopsy:** Low power view of the skin shows diffuse involvement of the dermis and deep subcutaneous tissues by a blue / basophilic infiltrate. The overlying epidermis is uninvolved. At higher power, we can see the infiltrate is comprised of medium to large cells with high N:C ratio and irregularly shaped nuclei.

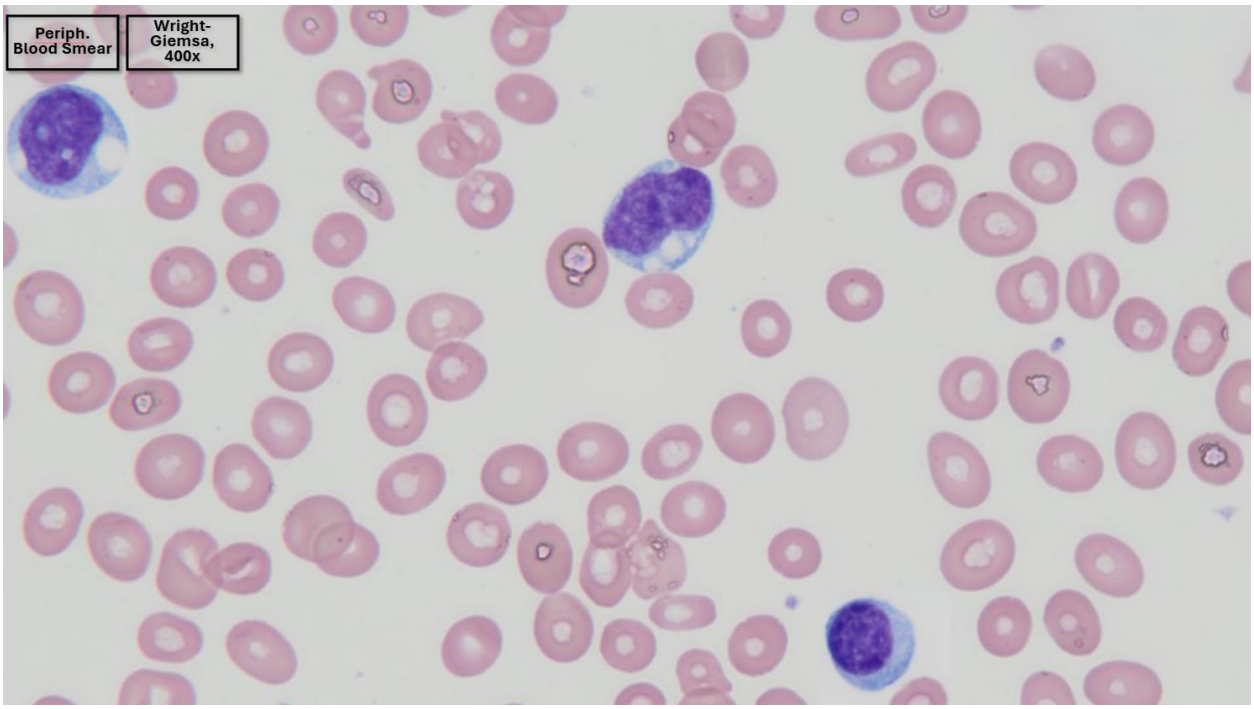

- **Peripheral Smear:** There is marked anemia and thrombocytopenia. In the top left and center of the image, there are circulating lesional cells which are larger in comparison to the lymphocyte present. These lesional cells demonstrate irregularly shaped nuclei with variably fine chromatin and inconspicuous nucleoli. Their cytoplasm is slightly basophilic to pale blue and contains cytoplasmic vacuoles of varying sizes. Overall, the morphology appears similar to what was seen in the patient's skin.

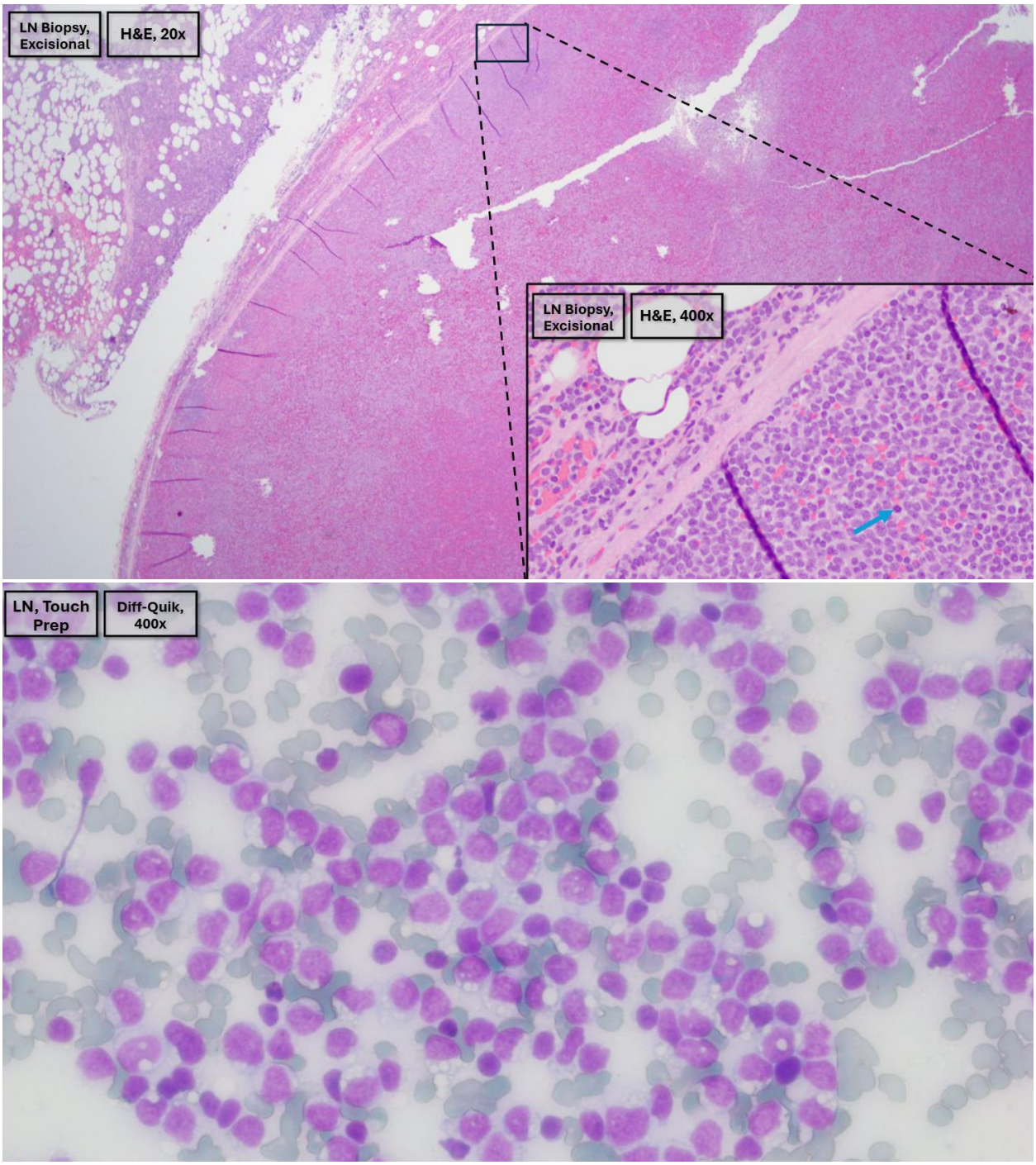

- **Lymph Node:** At low power, there is diffuse effacement of normal lymph node architecture with extension of the lesion outside the lymph node capsule. Higher power reveals the same monotonous population displaying blastoid morphology. Mitotic figures are readily visualized. Touch preparations of the lymph node show that the morphology of the neoplastic cells is similar to that seen in the peripheral blood, with monotonous medium to large-sized cells displaying fine chromatin and cytoplasmic vacuoles.

Immunophenotype by Flow Cytometry and IHC Staining:

Positive Markers:	Negative Markers:
CD33	MPO
CD2	CD34
HLADR	Surface CD3 and cytoplasmic CD3
CD123	CD19
CD4	CD14
CD56	CD64
CD303	CD11c
TCL1a	Lyzozyme
	MPO
	CD1a

Discussion:

Blastic plasmacytoid dendritic cell neoplasm (BPDCN) is a rare, aggressive hematologic malignancy derived from plasmacytoid dendritic cell precursors. This entity can present significant diagnostic challenges. Its distinction from other blastoid hematopoietic entities such as acute myeloid leukemia (AML) requires careful attention to morphology, immunophenotyping, and molecular features.

BPDCN, while a rare disease, typically presents in older male patients. It is commonly characterized by disseminated, extramedullary involvement with common sites including skin, lymph nodes, bone marrow, or CSF. In particular, skin lesions are a common presenting feature of BPDCN and are described as deep purple to red-brown macules, plaques, or tumors. Histopathology shows diffuse, monomorphic cells with irregular nuclei, fine chromatin, and scant, agranular cytoplasm. Overall, the cells typically display a blastoid morphology with eccentric nuclei and may show delicate wispy cytoplasmic extensions (pseudopodia) and cytoplasmic microvacuoles (“string of pearls”).

The distinction between BPDCN and AML, particularly AML with monocytic differentiation or AML with plasmacytoid dendritic cell differentiation (pDC-AML), is critical, as they can share overlapping immunophenotypic markers (CD4, CD56, CD123, HLA-DR). Diagnosis of BPDCN requires immunophenotypic evaluation with specific plasmacytoid dendritic cell (pDC) markers such as CD123, TCF4, TCL1, CD303, and CD304, along with CD4 and CD56. The diagnostic criteria given by the WHO specify either: (1) expression of CD4 and/or CD56 plus CD123 and one other pDC marker, OR (2) expression of any three pDC markers with absent expression of expected negative markers (CD3, CD14, CD19, CD34, lysozyme, myeloperoxidase). BPDCN is characterized by frequent mutations in TET2 (57%), ASXL1 (33%), NRAS (29%), SRSF2 (14%), and ZRSR2 (14%).

The prognosis of BPDCN is overall poor, with a median overall survival ranging from 8 to 24 months depending on the study. However, cases of pediatric BPDCN have been described to demonstrate less aggressive behavior and better response to chemotherapy as compared to their adult counterpart. Targeted treatment for BPDCN includes Tagraxofusp, which is drug consisting of a fusion protein consisting of interleukin 3 (IL-3) fused to diphtheria toxin. The fusion protein readily kills cultured pDCs by binding to their IL-3 receptor (CD123), thereby gaining entrance to the neoplastic cells and subsequently blocking the cells’ protein synthesis. Other regimens for treating BPDCN include regimens used for AML and B-ALL. For patients who can achieve initial remission, stem cell transplant is a viable treatment option.

Take home points:

BPDCN is a unique and aggressive neoplasm derived from pDC precursors with characteristic disseminated involvement; skin lesions are frequently the initial declaration of disease. BPDCN has a classic immunophenotype of "123456": CD123, CD4, CD56. However, as entities such as AML with monocytic differentiation have been described to display this phenotype, it is important to demonstrate the expression of other pDC markers (CD303,CD304, TCL1, TCF4) in order to make a definitive diagnosis of BPDCN. Ultimately, a multidisciplinary team is crucial for diagnosing and treating BPDCN and includes many members such as hematopathologists, dermatopathologists, cytopathologists, hematologists/oncologists, stem cell transplant staff, dermatologists, etc.

References:

1. Khoury JD, Takeuchi K, Pemmaraju N, et al. Blastic plasmacytoid dendritic cell neoplasm. In: WHO Classification of Tumours Editorial Board. Haematolymphoid tumours [Internet]. Lyon (France): International Agency for Research on Cancer; 2024 [cited 2026 01 10]. (WHO classification of tumours series, 5th ed.; vol. 11). Available from: https://tumourclassification.iarc.who.int/chapters/63.
2. Arber DA, Orazi A, Hasserjian RP, et al. International Consensus Classification of Myeloid Neoplasms and Acute Leukemias: integrating morphologic, clinical, and genomic data. Blood. 2022;140(11):1200-1228. doi:10.1182/blood.2022015850
3. Di Raimondo C, Lozzi F, Di Domenico PP, et al. Blastic Plasmacytoid Dendritic Cell Neoplasm, from a Dermatological Point of View. Int J Mol Sci. 2024;25(13):7099. Published 2024 Jun 28. doi:10.3390/ijms25137099
4. Fei F, Telatar M, Tomasian V, et al. Genetic characteristics of blastic plasmacytoid dendritic cell neoplasm: A single institution experience. Oncotarget. 2025;16:495-507. Published 2025 Jun 17. doi:10.18632/oncotarget.28742
5. Cuglievan, B., Connors, J., He, J. et al. Blastic plasmacytoid dendritic cell neoplasm: a comprehensive review in pediatrics, adolescents, and young adults (AYA) and an update of novel therapies. Leukemia 37, 1767–1778 (2023). https://doi.org/10.1038/s41375-023-01968-z
6. Shimony S, Luskin MR, Gangat N, LeBoeuf NR, Feraco AM, Lane AA. Blastic Plasmacytoid Dendritic Cell Neoplasm (BPDCN): 2025 Update on Diagnosis, Pathophysiology, Risk Assessment, and Management. Am J Hematol. 2025;100(8):1408-1422. doi:10.1002/ajh.27737
7. Jain A, Sweet K. Blastic Plasmacytoid Dendritic Cell Neoplasm. J Natl Compr Canc Netw. 2023;21(5):515-521. doi:10.6004/jnccn.2023.7026
8. Elizabeth L. Courville MV. Acute myeloid leukemia with mutated NPM1. ImageBank. Accessed February 1, 2026. https://imagebank.hematology.org/reference-case/6/acute-myeloid-leukemia-with-mutated-npm1.
9. Miranda RN, Medeiros J. Myeloid Sarcoma. ExpertPath. Accessed February 1, 2026. https://app.expertpath.com/document/myeloid-sarcoma/551f05bf-6941-4d58-9f5b-9611947094b7?term=myeloid+sarcoma&searchType=documents&category=All&documentTypeFilters=all.
10. Girish Venkataraman M. B-all blasts in blood. ImageBank. Accessed February 1, 2026. https://imagebank.hematology.org/image/61569/ball-blasts-in-blood?type=upload.

11. Sukswai N, Khoury J. Pathology outlines - blastic plasmacytoid dendritic cell neoplasm. Accessed February 1, 2026. https://www.pathologyoutlines.com/topic/bonemarrowneoplasticBPDCN.html.
12. Khanlari M, Young Ok C, Crane G. Pathology outlines - MCL-aggressive variants. Accessed February 1, 2026. https://www.pathologyoutlines.com/topic/lymphomaMCLaggressive.html.

Case #2:

Presenter: Havva Gokce Terzioglu, MD

Attendings: Guliz A. Barkan, MD and Phillip McMullen, MD, PhD

Diagnosis: Epithelioid Inflammatory Myofibroblastic Sarcoma

Clinical history:

The patient is a 58-year-old woman with a history of psoriasis and asthma who presented after a syncopal episode on a flight from Europe, followed by approximately one week of cough and shortness of breath. Computed tomography angiography of the chest was negative for pulmonary embolism but revealed a 5.0 cm mass in the right lung, along with tree-in-bud nodularities in the left lower lobe favored to represent infectious bronchiolitis. She was treated with antibiotics, resulting in resolution of respiratory symptoms; however, follow-up imaging demonstrated persistence of the right lung mass. Subsequently, transbronchial biopsy and needle aspiration and resection of the mass lesion were performed.

Morphology:

Transbronchial needle aspiration and biopsy: Smears showed limited viable material, consisting of squished cells with elongated nuclei in a background of lymphocytes. Diff-Quik–stained touch preparations demonstrated scattered spindle cells with elongated nuclei in an inflammatory background. At high magnification, the spindle cells exhibited vesicular chromatin, inconspicuous nucleoli, and variable cytoplasm. A satisfactory cell block was obtained, showing cohesive spindle to epithelioid cells in a lymphoplasmacytic background with focal necrosis. Transbronchial biopsy yielded lesional fragments and adjacent alveolated lung parenchyma. The morphology was similar to the cell block, with a more prominent plasma cell–rich inflammatory infiltrate.

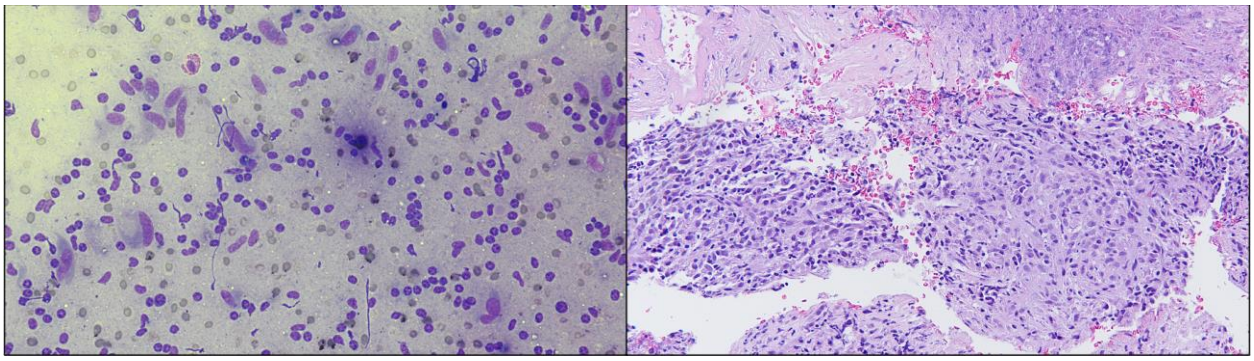

Resection: Right upper and middle lobectomy revealed a 7.3 × 5.2 cm tan-white, relatively well-circumscribed solid mass with foci of calcification and hemorrhage. Histologic sections showed areas resembling low-grade spindle cell morphology seen in the biopsy, as well as epithelioid areas composed of round to oval cells with prominent nucleoli and abundant granular cytoplasm. More advanced atypical features were present, including binucleation, hyperchromasia, increased mitotic activity, and extensive necrosis.

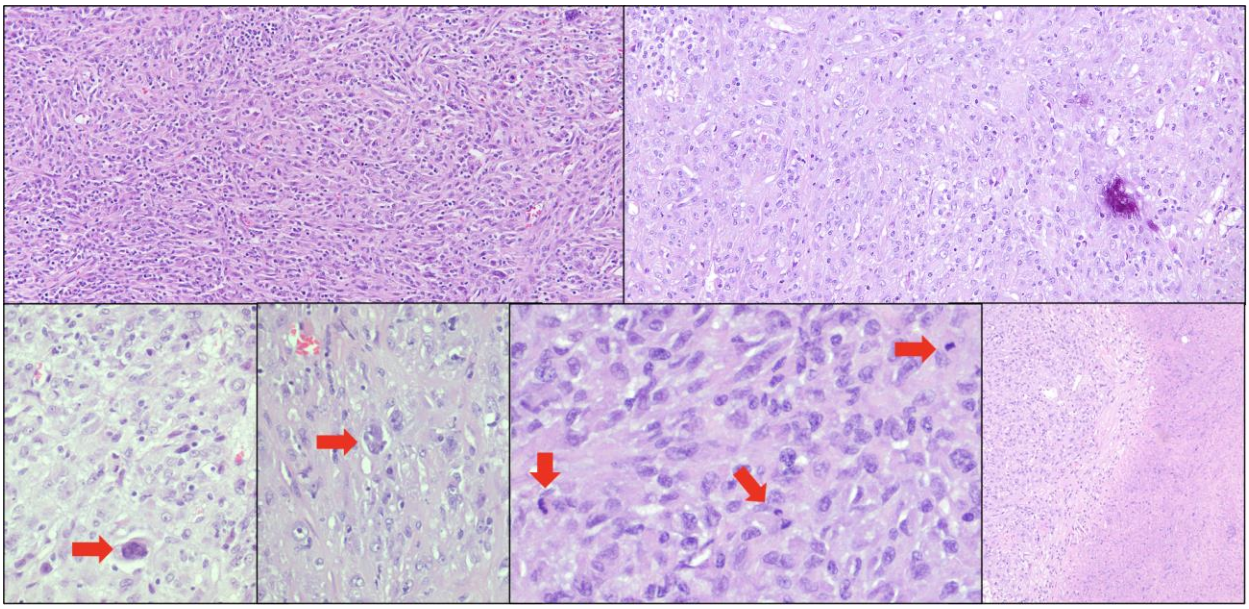

Differential diagnosis:

- Infectious or inflammatory pseudotumor
- Pleomorphic carcinoma
- Inflammatory myofibroblastic tumor (IMT) (with malignant transformation)
- Leiomyosarcoma
- EBV-positive inflammatory follicular dendritic cell sarcoma

Stains:

Category	Stains
Positive	ALK (diffuse), SMA (focal), Desmin (focal)
Negative	AE1/AE3, CK8/18, Calponin, S100, SOX10, CD21, CD23, OSCAR
Special stains	AFB (–), GMS (–)

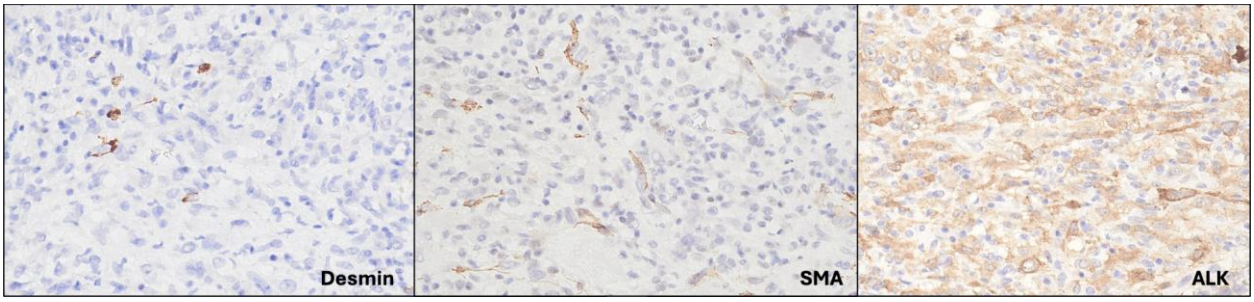

Molecular:

Comprehensive molecular testing identified:

- SQSTM1::ALK fusion

- TERT promoter mutation (C228T)

Discussion:

An infectious or reactive inflammatory pseudotumor was initially considered given the inflammatory background. However, special stains for microorganisms, including AFB and GMS, were negative, and there was no granulomatous inflammation. In addition, the tumor demonstrated diffuse ALK positivity, supporting a clonal neoplastic process rather than a reactive lesion. Pleomorphic (spindle cell) carcinoma was also considered due to the spindle cell morphology. However, the tumor cells were negative for epithelial markers, including AE1/AE3 and CK8/18, arguing against epithelial differentiation and excluding this diagnosis. Leiomyosarcoma was evaluated in the differential given the presence of bland spindle cells and focal expression of smooth muscle markers. However, SMA and desmin were only very focally positive, calponin was negative, and the presence of diffuse ALK positivity was not typical for leiomyosarcoma, making this diagnosis unlikely. EBV-positive inflammatory follicular dendritic cell sarcoma was considered due to the prominent lymphoplasmacytic background. However, the tumor cells were negative for follicular dendritic cell markers, including CD21 and CD23, the pulmonary location was atypical, and diffuse ALK positivity is not a feature of this entity, supporting its exclusion. The combination of spindle cell morphology, inflammatory background, and diffuse ALK positivity most strongly supported a diagnosis of inflammatory myofibroblastic tumor. However, the presence of cytologic atypia, increased mitotic activity, and necrosis raised concern for malignant transformation, which was subsequently confirmed on resection as epithelioid inflammatory myofibroblastic sarcoma.

Epithelioid inflammatory myofibroblastic sarcoma is a rare, high-grade malignant variant of inflammatory myofibroblastic tumor. First described in 2011, it is characterized by epithelioid morphology, near-universal ALK rearrangements, and aggressive clinical behavior with early recurrence and metastasis. Histologically, EIMS is composed of sheets of round to epithelioid cells with vesicular nuclei, prominent nucleoli, and abundant cytoplasm. A minor spindle cell component may be present. Increased mitotic activity and necrosis help distinguish EIMS from conventional IMT. Immunohistochemically, EIMS is almost always ALK positive, often with fusion partner–dependent staining patterns. Desmin is frequently positive, SMA is variable, and keratins are usually negative. Molecularly, ALK rearrangement is a defining feature, most commonly involving RANBP2 or RRBP1, with rare fusion partners such as SQSTM1. Pulmonary involvement by EIMS is extremely rare. Review of reported cases highlights the limited number of documented pulmonary examples and underscores the diagnostic challenges posed by this entity in the lung.

Learning points:

- Pulmonary spindle cell lesions have a broad differential diagnosis, including infectious, inflammatory, and neoplastic entities.
- Epithelioid inflammatory myofibroblastic sarcoma is a rare but aggressive malignant variant of IMT characterized by epithelioid morphology, necrosis, and ALK rearrangement.
- Accurate classification is critical, given the potential role of targeted therapy in ALK-driven neoplasms.
- Well-sampled cytology with cell block can yield highly representative material and often drive the diagnostic and molecular workup in challenging tumors.

References:

1. Androulaki A, Papathomas TG, Liapis G, et al. Inflammatory pseudotumor associated with Mycobacterium tuberculosis infection. Int J Infect Dis. Nov 2008;12(6):607-10. doi:10.1016/j.ijid.2007.12.011
2. Farris AB, 3rd, Kradin RL. Follicular localization of dendritic cells in a xanthomatous inflammatory tumor of lung associated with human herpes virus-8 infection. Virchows Arch. Dec 2006;449(6):726-9. doi:10.1007/s00428-006-0318-y
3. Coffin CM, Hornick JL, Fletcher CD. Inflammatory myofibroblastic tumor: comparison of clinicopathologic, histologic, and immunohistochemical features including ALK expression in atypical and aggressive cases. Am J Surg Pathol. Apr 2007;31(4):509-20. doi:10.1097/01.pas.0000213393.57322.c7
4. Mariño-Enríquez A, Wang WL, Roy A, et al. Epithelioid inflammatory myofibroblastic sarcoma: An aggressive intra-abdominal variant of inflammatory myofibroblastic tumor with nuclear membrane or perinuclear ALK. Am J Surg Pathol. Jan 2011;35(1):135-44. doi:10.1097/PAS.0b013e318200cfd5
5. Singh P, Nambirajan A, Gaur MK, et al. Primary pulmonary epithelioid inflammatory myofibroblastic sarcoma: a rare entity and a literature review. J Pathol Transl Med. Jul 2022;56(4):231-237. doi:10.4132/jptm.2022.05.08
6. Sunga CGG, Higgins MS, Ricciotti RW, Liu YJ, Cranmer LD. Inflammatory myofibroblastic tumor of the mesentery with a SQSTM1::ALK fusion responding to alectinib. Cancer Rep (Hoboken). Mar 2023;6(3):e1792. doi:10.1002/cnr2.1792
7. Yang L, Li P, Liu R, et al. Thoracic epithelioid inflammatory myofibroblastic sarcoma: a rare and aggressive disease with case report and literature review. Discov Oncol. Sep 27 2024;15(1):484. doi:10.1007/s12672-024-01375-5

IRAP Case #3

Presenter: Madelyn Traczek, DO

Attendings: Dr. Robert Pooley, MD; Dr. Phillip McMullen, MD, PhD

Clinical History:

A 23 year old Asian man with past medical history significant for polysubstance use including Ketamine (5-7 g/week), alcohol (2-4 drinks/week), and Tylenol for pain (4-5 tablets/day, dose unknown) presented to an outside hospital emergency department complaining of three days of abdominal pain, nausea, and dysuria. The patient reported to the clinical team that the recreational ketamine he purchased was frequently cut with “vitamins,” so it was unclear if any additional substances may have been consumed as a result. Labs upon presentation were significant for leukocytosis and transaminitis. Given the history provided, clinicians were concerned for drug-induced liver toxicity and the patient was treated with N-acetylcysteine. The patient failed to improve and as a result was transferred to Loyola University Medical Center (LUMC) four days after initial presentation for escalation of care and liver transplant evaluation. During transport the patient became hypoxic and tachypneic, requiring MICU admission for treatment of acute hypoxic respiratory failure. CT abdomen and pelvis taken shortly after arrival to LUMC showed an enlarged liver with nonspecific findings consistent with acute hepatitis, and lungs with bilateral ground-glass opacities and mild bilateral effusions, suspicious for multifocal pneumonia. The patient continued to decline rapidly, exhibiting signs of multi-organ failure with a steeply increasing white blood cell count and liver enzymes. The white blood cell count peaked at 49.4 on his second day of admission at Loyola. The patient’s CBC was also significant for thrombocytopenia which was contributed to the patient’s liver failure. Due to the patient’s status he was deemed not a candidate for liver transplant, and passed away shortly after family opted for transition to comfort care. An autopsy was requested by the family due to the patient's rapid decline upon presentation and lack of definitive etiology for his illness. An H&E slide of the right lung taken at time of autopsy is provided for review.

Final Diagnosis: Aggressive NK Cell Leukemia

Differential Diagnoses:

- Drug-Induced Acute Hepatic Failure
- Disseminated infection
    - Acute viral hepatitis
    - Pneumonia
- Nonspecific Interstitial Pneumonia
- Vasculitis
    - Polyarteritis nodosa
    - Granulomatosis polyangiitis
    - Microscopic polyangiitis
- Hematopoietic Malignancy
    - Chronic lymphocytic leukemia
    - B-lymphoblastic leukemia
    - T-lymphoblastic leukemia
    - Intravascular large B-cell lymphoma
    - Mature T cell and NK cell neoplasms

Histopathology:

At the time of autopsy, hepatomegaly with a liver weight of 4,060 g (normal expected 1400-1910 g) was observed consistent with the patient's antemortem imaging. The liver had a smooth, mottled external surface (A) and the cut surface showed prominent red-brown congestion (B). The only other significant gross finding was diffuse congestion of the bilateral lungs, with no grossly observable lesions or consolidations.

Upon histological examination, representative sections of the lungs showed alveolar hemorrhage, hyaline membrane formation, and diffuse cellular interstitial infiltrates (C). The infiltrates demonstrate a perivascular distribution, while also involving the alveolar walls. The cellular infiltrate consists of a monomorphic population of mononuclear cells, consistent with a lymphoid population (D). Multiple sections of the myocardium demonstrate a similar population of monotonous mononuclear cells concentrated in the perivascular space with infiltration into the myocardial interstitium (E). Sections of the liver demonstrate widespread necrosis and prominent congestion throughout, again with diffuse mononuclear cell infiltrates consistent with those observed in the lungs and heart (F).

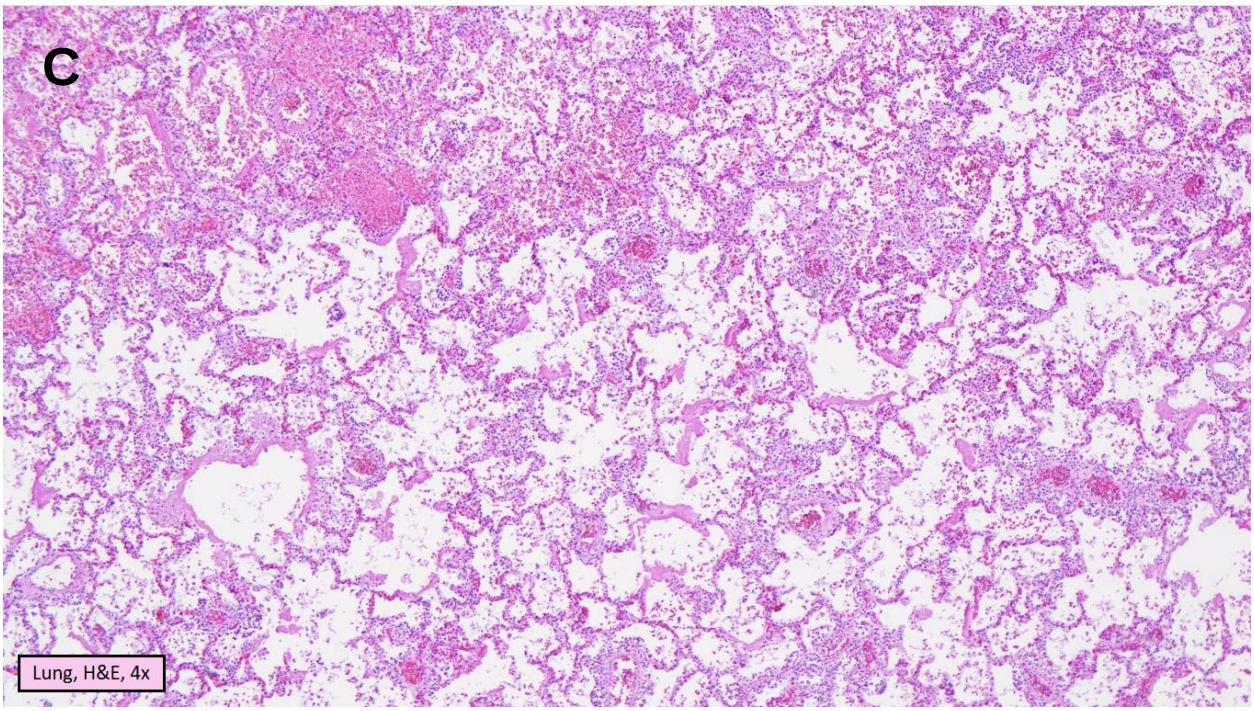
C
Lung, H&E, 4x

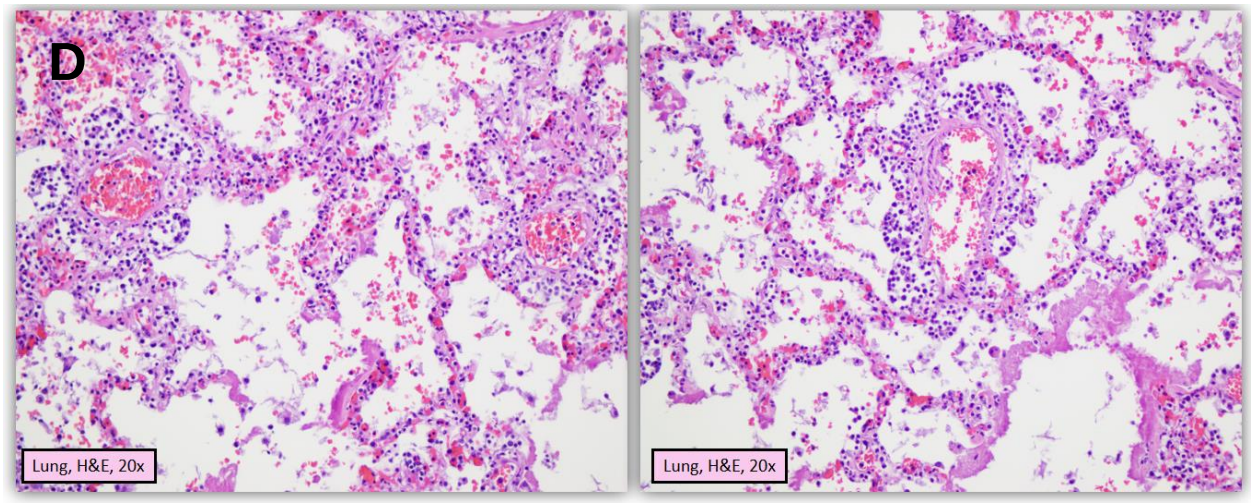
D
Lung, H&E, 20x
Lung, H&E, 20x

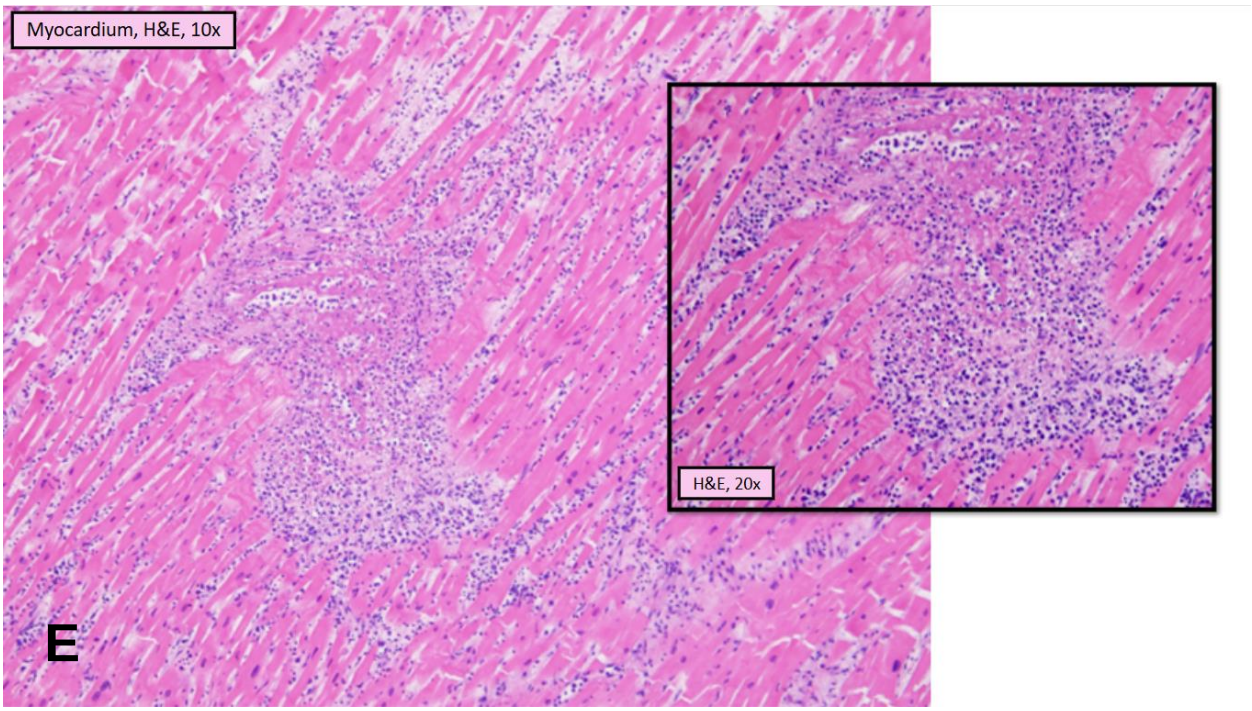

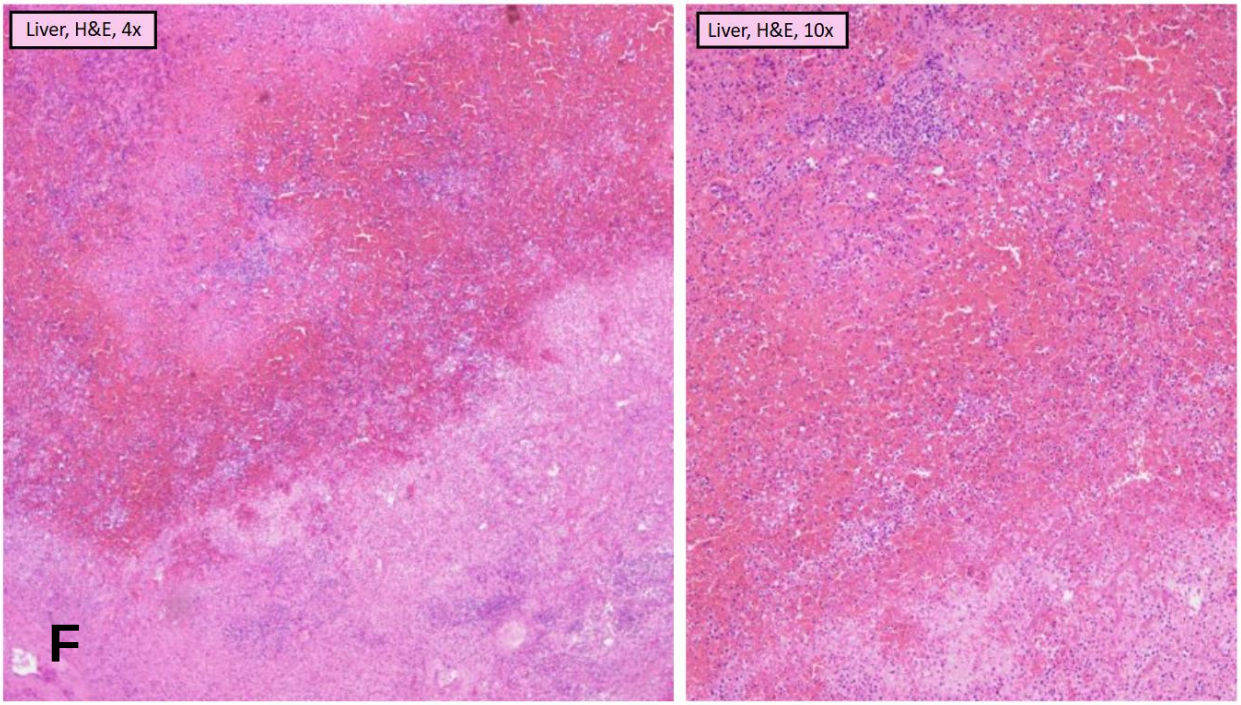

A panel of immunohistochemical stains were performed on sections of lung to characterize this multi-organ cellular infiltrate. CD3, CD8, and CD56 stains demonstrated diffuse positivity within our cells of interest (G). CD20, CD4, CD34, and EBER were negative in the population of interest. Due to this staining pattern in combination with the patient's clinical presentation, this entity was diagnosed as Aggressive NK Cell Leukemia.

G.

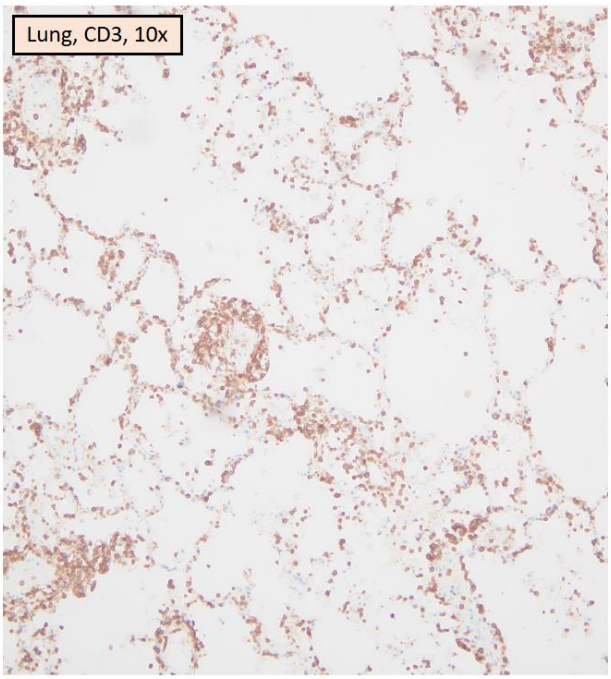

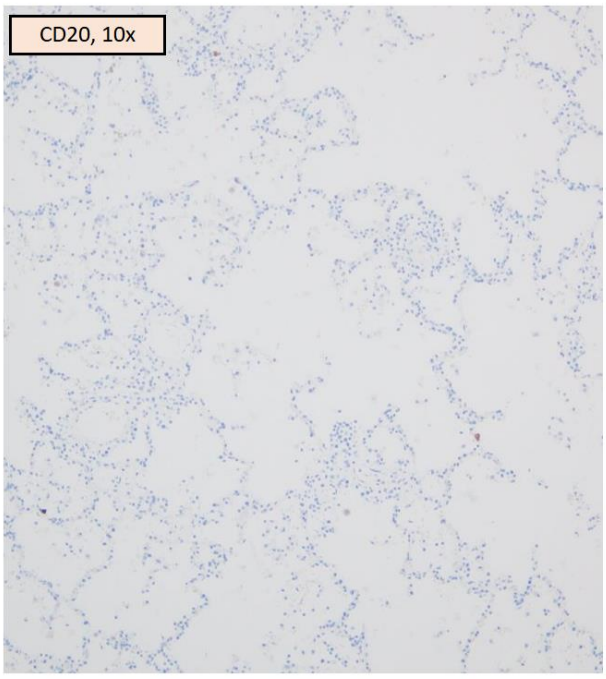

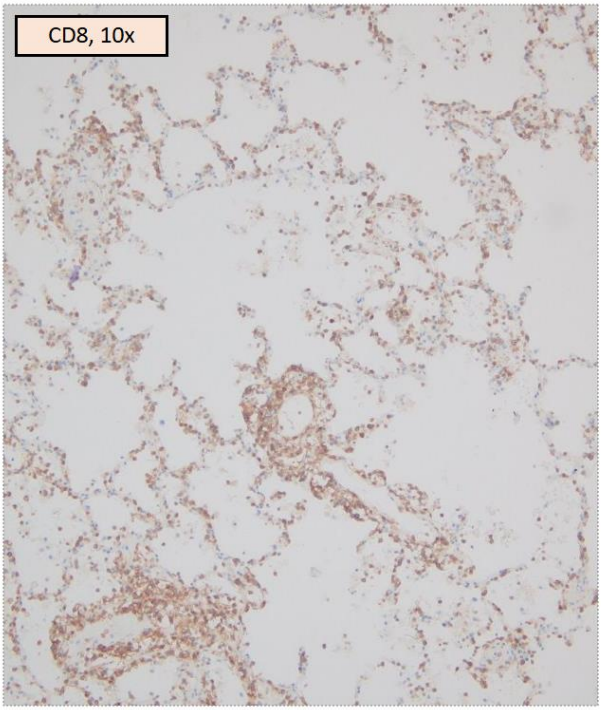

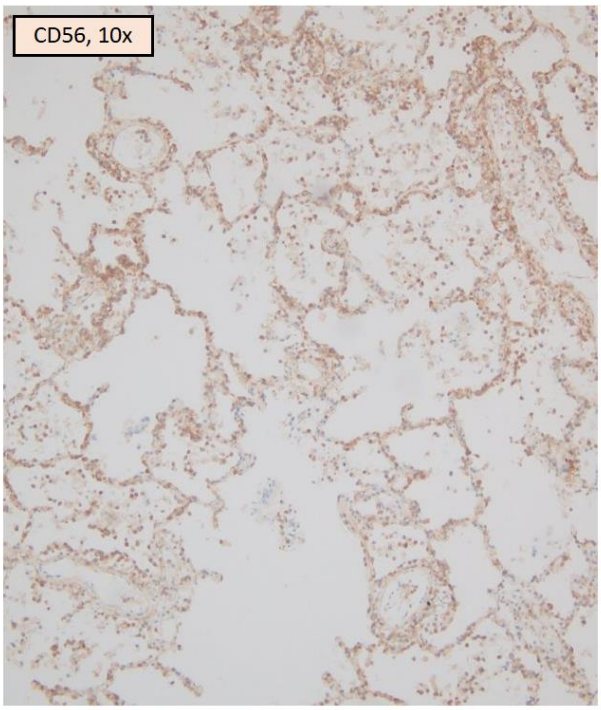

Discussion:

Aggressive NK Cell Leukemia (ANKL) is a rare leukemia of unknown etiology, although it has a strong association with EBV, with EBV positivity reported in about 90% of cases. Though our EBV stain was negative, it is possible this was a false negative due to a low quality postmortem specimen. Even in the case of a true negative EBV result, there is still a small subset of ANKL cases which are EBV negative so this does not preclude this diagnosis. This entity is most common in Asian populations, and typically affects young to middle age patients with a median age of 40 years, fitting with our patient's demographic.

ANKL commonly involves the peripheral blood, bone marrow, liver, and spleen, and presentation includes fever, constitutional symptoms, leukemic blood picture, and hepatosplenomegaly sometimes accompanied by abnormal liver function tests and jaundice. The presentation can sometimes mimic hepatitis, such as in our patient. Unfortunately this is a very aggressive neoplasm with a typically fulminant clinical course resulting in multiorgan failure, and reported median survival is less than 7 months.

Morphology of ANKL typically demonstrates a monotonous population of leukemic cells within the peripheral blood. At the organ sites it shows diffuse to patchy destructive infiltrates morphology ranging from round and bland to irregularly folded pleomorphic nuclei with condense chromatin and small nucleoli. Positive markers that can be useful in making this diagnosis include CD2, cytoplasmic CD3, CD16, CD56, perforin A, granzyme B, and EBER (most cases). MYC, BCL2, and p53 also frequently show positivity. CD3, CD4, CD5, CD57, and T cell receptors are typically negative. Flow cytometry is beneficial for diagnosis, but unfortunately no specimen was available from this patient to perform flow cytometry following the autopsy.

Treatment of this neoplasm includes allogenic hematopoietic stem cell transplant, which can improve outcomes for patients but often only confers benefit for a limited period of time. There is currently no consensus on chemotherapeutic regiments for ANKL, however regimens that include L-asparginase such as SMILE (dexamethasone, methotrexate, ifosfamide, etoposide and L-asparaginase), AspaMetDex (L-asparaginase, methotrexate and dexamethasone), and VIDL (etoposide, ifosfamide, dexamethasone and L-asparaginase) have shown some benefit.

Take Home Points:

- Aggressive NK Cell Leukemia is a rare but aggressive entity, and though treatment options are limited, they can extend patient survival time, making prompt diagnosis important.
- Given our patient's rapid decline, it is impossible to say whether an antemortem diagnosis could have improved his chance of survival, however performing flow cytometry on a peripheral blood sample could have provided the information needed to make the diagnosis in a shorter timeframe and therefore give the patient's family the closure they desired sooner.
- Given the patient's history of polysubstance abuse, the clinical team was very focused on treatment of drug-induced liver toxicity. This case reminds us that one should not assume that all problems must be drug-related in a patient with a history of drug use, and reminds us of the importance of considering a broad differential rather than anchoring on any single diagnosis.

References:

1. El Hussein S, Khoury J. Aggressive NK cell leukemia. PathologyOutlines.com website. https://www.pathologyoutlines.com/topic/lymphomanonbnkcell.html. Accessed January 12th, 2026.
2. El Hussein S, Medeiros LJ, Khoury JD. Aggressive NK Cell Leukemia: Current State of the Art. Cancers (Basel). 2020 Oct 9;12(10):2900. doi: 10.3390/cancers12102900. PMID: 33050313; PMCID: PMC7600035.
3. Fyfe, B. S. (2024, March 20). Vasculitis. ExpertPath. https://app.expertpath.com/document/vasculitis/4fb24e03-a2c1-4a87-b7f1-6a55d32c3e1c?term=vasculitis&searchType=documents&category=All&documentTypeFilters=all
4. Kakar, S. (2021, July 8). Drug-Induced Acute Hepatic Failure. ExpertPath. https://app.expertpath.com/document/drug-induced-acute-hepatic-failure/dcfc50fb-4c6b-466d-b066-3d2e5350d57f?term=Drug-

Induced+Acute+Hepatic+Failure&searchType=documents&category=All&documentTypeFilters=all

5. Sumbly V, Vest M, Landry I. Aggressive Natural Killer Cell Leukemia: A Brief Overview of Its Genomic Landscape, Histological Features, and Current Management. Cureus. 2022 Feb 23;14(2):e22537. doi: 10.7759/cureus.22537. PMID: 35345687; PMCID: PMC8956279.
6. Suster, D. I., Mino-Kenudson, M., & Suster, S. (2021, December 1). Nonspecific Interstitial Pneumonia. ExpertPath. https://app.expertpath.com/document/nonspecific-interstitial-pneumonia/33cc14b9-d299-423e-8a5f-310d31680a7e.
7. Suzuki, R., Ott, G., Takeuchi, K., Cheng, C. L., Loughran, T. P., Khoury, J. D., Ng, S.-B., Yamaguchi, M., & Kwong, Y.-L. (2026). Aggressive NK Cell Leukemia. World Health Organization. https://tumourclassification.iarc.who.int/chaptercontent/63/257.
8. Yoshikawa A, Bychkov A. ARDS / DAD. PathologyOutlines.com website. https://www.pathologyoutlines.com/topic/lungnontumordiffusealveolardamage.html. Accessed February 5th, 2026.

Presenter: Leah Gruen, MD

Mentors: Phillip McMullen, MD PhD and Guliz Barkan, MD

Clinical History:

A 55-year-old male who is a current smoker with a 40-pack-year smoking history presented with an acute onset of left-sided chest pain. He denied fevers, chills, shortness of breath, cough, night-sweats, weight loss, or any other constitutional symptoms. A CT of the chest showed an 11 cm left anterolateral mediastinal mass. The patient initially underwent an FNA and transbronchial biopsy of the mass, and later a complete resection.

Final Diagnosis: Giant hamartoma

Differential diagnosis 1 (following FNA & biopsy):

- Papillary adenocarcinoma
- Sclerosing pneumocytoma
- Well-differentiated papillary mesothelial tumor
- Mesothelioma with papillary growth pattern
- Ciliated muconodular tumor/bronchiolar adenoma

Differential diagnosis 2 (following resection):

- Pulmonary blastoma
- Intrapulmonary teratoma
- Carcinosarcoma
- Pleomorphic adenoma

Key Features:

Histopathology: Histologic examination of the FNA biopsy (A), and resection (B and C) specimens taken together show a well-circumscribed biphasic neoplasm comprised of relatively bland epithelial components with glandular and papillomatous architecture and mesenchymal components including cartilage, adipose tissue, smooth muscle, and a myxoid stroma. There is central calcification, and foci of cystic degeneration and hemorrhage. The cytologic features of the epithelial component vary with some areas showing monotonous columnar cells arranged in invaginating glandular structures, while other areas show flattened-to-cuboidal cells with mild nuclear pleomorphism. There is no definitive evidence of lymphovascular invasion. No prominent mitoses nor tumor necrosis are identified.

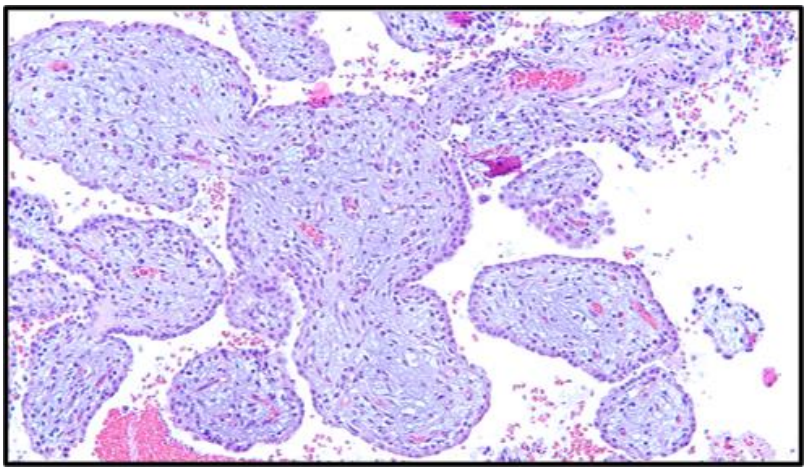

(A)

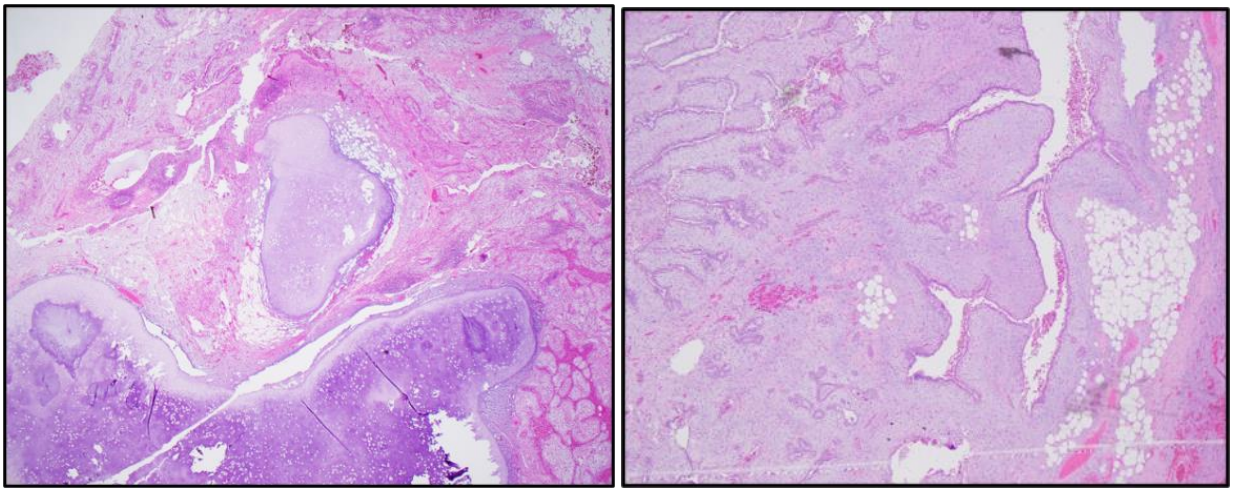

(B)

A large panel of immunohistochemical stains were performed and summarized in the chart below. Notably, the epithelial component is positive for a KeratinAE1/AE3, Napsin A, and TTF-1, demonstrating a pulmonary-derived epithelial component. P40 highlighted focal basal cells in the epithelial component. Beta-catenin showed focal nuclear and cytoplasmic positivity with predominantly membranous staining of the epithelial cells. Mesothelial markers WT1 and calretinin were negative. GFAP, SMA, and S100 did not highlight a myoepithelial component. S100 showed variable staining most prominent in the cartilaginous and lipomatous stromal components. Ki-67 was <1%.

IHC	Epithelial component	Stromal component
Keratin AE1/AE3	+	-
CK5/6	+	-
TTF-1	+	-

Napsin A	+	-
EMA	+	-
p40	+ focally	-
WT1, Calretinin	-	-
GFAP	-	-
S100	-	Variable, most prominent in cartilaginous and lipomatous differentiation
Beta-catenin	Focal nuclear and cytoplasmic with predominantly membranous staining	-
Ki-67	<1%	<1%

Molecular: Molecular testing (MayoComplete Solid Tumor Panel) was performed at Mayo Clinic Laboratories and no clinically relevant variants, fusions, or splice/transcript variants were identified with adequate coverage of the assessed genes.

Discussion:

Pulmonary hamartomas are the most common benign lung neoplasms in adults, with the majority ranging in size from 1.6-2.9 cm. Giant pulmonary hamartomas, considered those >8 cm, are exceedingly rare, with less than 25 reported cases in the English literature (1). While typical pulmonary hamartomas usually present asymptomatically as incidental findings, patients with giant hamartomas frequently present with pulmonary-related symptoms (1). Histologically, pulmonary hamartomas are composed of varying amounts of mesenchymal components including connective tissue, fat, cartilage, and smooth muscle, with entrapped respiratory epithelium. Pulmonary hamartomas are generally considered benign entities. However, there have been rare case reports of hamartomas with malignant transformation, almost exclusively occurring in giant hamartomas. Reported cases have shown giant pulmonary hamartomas with malignant transformation to liposarcoma (2), squamous cell carcinoma (3), chondrosarcoma (4), and leiomyosarcoma (5). These cases highlight the importance of due diligence in ruling out malignant components arising from giant hamartomas, and routine clinical follow-up for these patients.

Take home points:

- Giant pulmonary hamartomas are rare entities and while generally considered benign, do have the potential for malignant transformation
- When the clinical features (11 cm lung mass in a smoker) and the potential diagnosis (benign hamartoma) appear at odds, it's important to do a comprehensive work-up
- Well-sampled cytology with cell block can yield highly representativematerial that can drive the diagnostic work-up in challenging cases
- The biopsy is not always representative of the entirety of a lesion

1. Fan X, Breaux B, Leonards L, Mirza R. A rare case of asymptomatic giant pulmonary hamartoma. Diagn Pathol. 2024 Jun 22;19(1):87. doi: 10.1186/s13000-024-01506-0. PMID: 38909245; PMCID: PMC11193182.
2. Siblani, D., Kanj, M., Ghorra, C., Haddad, Y., Jomaa, M., & Mansour, Z. (2022). A Liposarcoma Arising in a Pulmonary Hamartoma, Coexisting With Benign Metastasizing Leiomyoma. The Annals of Thoracic Surgery, 113(3), e203–e205. https://doi.org/10.1016/j.athoracsur.2021.05.021
3. Lee BJ, Kim HR, Cheon GJ, Koh JS, Kim CH, Lee JC. Squamous cell carcinoma arising from pulmonary hamartoma. Clin Nucl Med. 2011;36(2):130–131. doi: 10.1097/RLU.0b013e318203bc27
4. Schenkel R, Altfillisch C, Chung J, Verma A, Balters M. Malignant Degeneration of Biopsy-Proven Hamartoma to Chondrosarcoma. Cureus. 2020 Dec 18;12(12):e12150. doi: 10.7759/cureus.12150. PMID: 33489562; PMCID: PMC7814419.
5. Luca S, Montella M, Monti R, Accardo M, Savarese G, Sirica R, et al. Pulmonary leiomyosarcoma arising in pulmonary hamartoma: an exceptional occurrence in a rare tumor. Pathologica. 2023;115(6):325–332. doi: 10.32074/1591-951X-941.